INL/JOU-21-61634-Revision-0

Halogenation of Used Aluminum Matrix Test Reactor Fuel -- A Bench-Scale Demonstration with Surrogate Materials

October 2021

Steven D Herrmann, Haiyan Zhao, Meng Shi, Matthew M Jones, Michael N Patterson

Changing the World's Energy Future

Idaho National Laboratory

INL is a U.S. Department of Energy National Laboratory operated by Battelle Energy Alliance, LLC

INL/JOU-21-61634-Revision-0

Halogenation of Used Aluminum Matrix Test Reactor Fuel -- A Bench-Scale Demonstration with Surrogate Materials

Steven D Herrmann, Haiyan Zhao, Meng Shi, Matthew M Jones, Michael N Patterson

October 2021

Idaho National Laboratory
Idaho Falls, Idaho 83415

http://www.inl.gov

Prepared for the
U.S. Department of Energy
Under DOE Idaho Operations Office
Contract DE-AC07-05ID14517

Halogenation of Used Aluminum Matrix Test Reactor Fuel – A Bench-Scale Demonstration with Surrogate Materials

Steven D. Herrmann[a,b,*], Haiyan Zhao[b], Meng Shi[b], Matthew M. Jones[a], Michael N. Patterson[a]

[a] Idaho National Laboratory, Idaho Falls, Idaho, USA

[b] University of Idaho, Idaho Falls, Idaho, USA

*Corresponding author; Tel: +1 208 533 7859; Email address: Steven.Herrmann@inl.gov; Postal address: P.O. Box 1625, Idaho Falls, Idaho, 83415-6180, USA

Halogenation of Used Aluminum Matrix Test Reactor Fuel – A Bench-Scale Demonstration with Surrogate Materials

Abstract

A series of experiments with surrogate materials was performed at bench scale to demonstrate a halogenation technique applicable to the treatment of used aluminum matrix test reactor fuel. The technique involves the dissolution and separation of aluminum from used aluminum matrix test reactor fuel in molten-halide salt systems, as a head-end step to the subsequent treatment and disposition of the fuel's uranium and fission products. The demonstration of the halogenation technique was performed with neodymium metal as a non-radiological surrogate for uranium metal. The experiments involved blending and heating forms of aluminum and neodymium metal with ammonium and lithium chloride or ammonium and lithium bromide. The sublimation and decomposition of ammonium chloride or bromide yielded ammonia gas along with the respective hydrogen chloride or bromide gas, the latter of which reacted and formed the respective aluminum and neodymium halides. At elevated temperatures, aluminum halides gasified and separated from the respective neodymium halides, which fused with their respective lithium halides. Samples of the fused and distillate salts were collected during the series of experiments and analyzed, yielding the extents of aluminum removal that ranged from 94.5–98.2% for chlorination runs and 91.4–97.8% for bromination runs. No neodymium was detected in any of the distillation fractions. Some experiments were repeated to verify the effectiveness, and a portion of aluminum chloride distillate was processed into a consolidated waste form.

Key words: aluminum matrix fuel, halogenation, aluminum and neodymium separation, ammonium chloride, ammonium bromide, lithium chloride, lithium bromide.

Introduction

Aluminum matrix fuels are widely used in materials test reactors throughout the world, including the Advanced Test Reactor (ATR) at Idaho National Laboratory. ATR is fueled with a total of 40 high-enriched uranium (HEU) driver elements that are uniquely arranged in a four-leaf-clover configuration to facilitate concentrated neutron densities within designated regions of the core, as illustrated in Figure 1. [1] Each individual driver element is composed of 19 curvilinear fuel plates of different widths, isometric and cross-sectional views of which are also shown in Figure 1. [2]

The fuel in each of the curvilinear plates is a uranium aluminide-aluminum dispersion matrix. Specifically, HEU metal and aluminum metal are melted, cast, and sized into a uranium aluminide powder, typically consisting of UAl_3 (63 wt%), UAl_4 (31 wt%), and UAl_2 (6 wt%) and commonly referred to as UAl_x. [3] The uranium aluminide powder is dispersed in aluminum metal powder and clad with 6061 aluminum alloy in a hot roll-bonding process. During the hot rolling and associated annealing steps, almost all the UAl_2 reacts with excess aluminum from the matrix to form UAl_3, and some UAl_3 reacts to form UAl_4. Consequently, the UAl_x in the final ATR fuel matrix consists of UAl_3 (60 wt%) and UAl_4 (40 wt%) with uranium densities up to 1.7 g/cc. [4]

The typical burnup of ATR HEU fuel is 40% [5], which, for nominal ATR operations, results in the generation rate of 30 or more used ATR fuel elements per year. [6] Used ATR fuel elements are temporarily stored in underwater racks and then dry storage racks near the reactor

site, while awaiting an ultimate disposition path that may include treatment in a dedicated facility or disposal in a repository. [6] To date, thousands of used ATR fuel elements have accumulated in wet and dry storage areas at Idaho National Laboratory.

As a metal fuel, used ATR fuel would appear to be well-suited for an established electrometallurgical treatment (EMT) process, which was developed by researchers at Argonne National Laboratory in the mid-1990s for treating sodium-bonded used metal fuel from fast reactors within the DOE complex and continues to operate today. The EMT process encompasses a series of unit operations to condition used sodium-bonded HEU fuel into a refined low-enriched uranium metal product, while fission products are directed into ceramic and metallic waste forms for disposal. [7–9] An extension of an EMT process has been proposed for used ATR fuel; [9] however, it is complicated by the presence of aluminum in a uranium electrorefining system. Specifically, uranium and aluminum form stable intermetallic compounds, as indicated by elevated melting points in an Al-U binary phase diagram (see Figure 2) and the following formation reactions. [10]

$$U + 2\ Al \rightarrow UAl_2 \qquad \Delta G_{f,500C} = -91.203\ kJ/mol \qquad (1)$$

$$U + 3\ Al \rightarrow UAl_3 \qquad \Delta G_{f,500C} = -104.656\ kJ/mol \qquad (2)$$

$$U + 4\ Al \rightarrow UAl_4 \qquad \Delta G_{f,500C} = -129.587\ kJ/mol \qquad (3)$$

The high thermodynamic stabilities of uranium aluminide compounds result in overpotentials that are needed to effect their anodic dissolution in an EMT uranium electrorefining system. Conversely, a uranium cathode would create an underpotential for aluminum metal deposition in the same system. Consequently, uranium and aluminum would tend to co-dissolve at the anode and co-deposit at the cathode in a uranium electrorefining

system, as defined for the EMT process. Indeed, the co-dissolution of uranium-aluminum and consequent inability to separate uranium from aluminum in a uranium electrorefining system was observed in a separate experimental study. [12]

To effectively separate and recover HEU from used ATR fuel in an EMT process, it is generally understood that a head-end step is required to first remove the aluminum component. Researchers at Argonne National Laboratory proposed and demonstrated an approach to remove aluminum from a uranium-aluminum alloy by (1) adding silicon to the alloy, (2) selectively electrorefining away aluminum in a fluoride electrolyte, and (3) recovering uranium via electrorefining in a separate electrorefiner with a different fluoride electrolyte. [13–16] Results from this demonstration were limited to the aluminum electrorefining step, where uranium concentrations in the aluminum cathode product ranged from 0.05–6 wt% while aluminum concentrations in the original U-Al-Si alloy ranged from 5.2–14.7 wt%.

While not related to the EMT of used ATR fuel, researchers from the European Union (EU) used aluminum as a cathode in a uranium electrorefiner to exploit the thermodynamic stability and associated co-deposition of not only uranium but also transuranium metals onto an aluminum metal cathode in a chloride electrolyte. [17–20] The use of an aluminum cathode to form actinide-aluminum alloys in a uranium electrorefiner has an advantage in an improved separation of actinides from lanthanides over other reactive cathodes, such as a liquid cadmium cathode. However, an additional step is required to separate and recover actinides from the actinide-aluminum alloy, which the same EU researchers demonstrated using chlorination. They conducted experiments with uranium-aluminum alloys that were exposed to pure chlorine gas [17–19] and hydrogen chloride gas [20]. Specifically, they conducted several experiments with the chlorination of gram and sub-gram quantities of pulverized UAl_3/UAl_2 with varying extents

of excess pure chlorine gas in a range of 150–170°C, yielding a UCl_4/UCl_3 and $AlCl_3$ product per the following reaction mechanisms.

$$U + x/2\ Cl_2\ (g) \rightarrow UCl_x \quad (4)$$

$$Al + 3/2\ Cl_2\ (g) \rightarrow AlCl_3 \quad (5)$$

Under these conditions, extents of uranium-aluminum chlorination approaching 99.8% were achieved over a 40-hour exposure period in a pass-through system. Operations at 150°C were preferred to preclude the formation of unwanted volatile UCl_5, traces of which were observed at 170°C. Once the alloy was chlorinated, the mixed UCl_x-$AlCl_3$ product could be heated above 180°C, at which temperature $AlCl_3$ sublimes [21] and separates from UCl_x.

Similar studies by some of the same EU researchers using HCl gas were conducted, based on the following reaction mechanisms.

$$U + x\ HCl\ (g) \rightarrow UCl_x + x/2\ H_2\ (g) \quad (6)$$

$$Al + 3\ HCl\ (g) \rightarrow AlCl_3 + 3/2\ H_2\ (g) \quad (7)$$

The use of HCl gas to chlorinate UAl_3/UAl_2 afforded higher operating temperatures (300–400°C), as the hydrogen gas product suppressed the formation of unwanted volatile UCl_5 or UCl_6. Also, chlorination at 300–400°C resulted in the simultaneous sublimation of $AlCl_3$. Essentially complete UAl_3/UAl_2 chlorination and $AlCl_3$ sublimation were observed at 300°C, while less favorable results were observed at 350 and 400°C.

The favorable results achieved by EU researchers with the chlorination and separation of aluminum from actinides in the proposed use of an aluminum cathode in a uranium electrorefiner suggest that such an approach could be applicable to used aluminum matrix fuels, including used

ATR fuel. Indeed, researchers at the Comision Nacional de Energia Atomica of Argentina proposed the chlorination of used aluminum-uranium fuel in their country with chlorine gas as high as 500°C to convert all constituents in the used fuel to their respective chlorides and to separate volatile aluminum chloride. [22] However, their proposal and accompanying theoretical study have not been experimentally validated.

The objective of this study was to demonstrate a halogenation technique that could be applied to separate aluminum from the used aluminum matrix ATR fuel in molten-halide salt systems, as a head-end step to subsequent treatment and disposition of the fuel's uranium and fission products. To simplify the demonstration, neodymium metal was used as a non-radiological surrogate for uranium metal, as neodymium forms a trivalent chloride of similar thermodynamic stability and vapor pressure to that of uranium. Furthermore, ammonium halides were used as the halogenating agents to avoid installation of a gaseous halogenation system. Accordingly, forms of aluminum and neodymium metal were blended at bench scale with either ammonium chloride or bromide and lithium chloride or bromide, respectively, and heated. Under these conditions, ammonium chloride and bromide sublime at 338 and 396°C, respectively, [21] decomposing into ammonia and hydrogen chloride and hydrogen bromide gases, respectively. The hydrogen halide gases react with aluminum and neodymium metal to form their respective halides. The overall generalized reaction mechanism is as follows.

$$M + 3\ NH_4X \rightarrow MX_3 + 3\ NH_3\ (g) + 3/2\ H_2\ (g) \qquad (8)$$

where M is aluminum or neodymium metal and X is chlorine or bromine.

As the aluminum halides form primarily above their respective sublimation point (180°C for aluminum chloride) and normal boiling point (255°C for aluminum bromide), [21] they gasify

and separate from the respective neodymium halides, which then fuse with their respective lithium halides. To determine the effectiveness of this halogenation technique, researchers analyzed the fused salt and distillate product samples, identifying the extents of aluminum and neodymium separation. As the generated aluminum halide would require a separate disposal pathway, the aluminum chloride distillate from one of the runs in this demonstration was treated to form a more durable, less soluble product by reacting it with magnesium oxide to convert the aluminum chloride to an insoluble aluminum oxide. The treated aluminum chloride distillate is referred to here as a waste-form product.

Experimental Aspects

Approach

As aluminum matrix ATR fuel is formed from metal powders that are hot rolled with aluminum cladding, this demonstration used neodymium and aluminum metal powders as surrogate forms of feed materials in a series of halogenation experiments. Aluminum foil was also added to some of the runs, representing the form of cladding in used ATR fuel. Lithium chloride and bromide were used as the primary diluents in the salt phases of this demonstration. The experiments involved blending ten parts by mass of the select lithium halide to one part neodymium metal powder and one part aluminum metal powder and, for a subsequent run, one part aluminum metal foil at a scale of 50 g of lithium halide. Sufficient ammonium halide was added to each blend to accommodate a 10% excess stoichiometric amount of halogen for the given masses of neodymium and aluminum metals in a run. Accordingly, a nominal 50 g of lithium chloride was blended in a glass jar with 5 g of neodymium powder, 5 g of aluminum powder, and 39 g of ammonium chloride for the first run. The blend was then transferred into a glassy carbon crucible, which was covered with an off-gas trap and heated in a furnace to

approximately 500°C at 10°C/hr to sublimate the ammonium chloride and thereby chlorinate the neodymium and aluminum metals per Eq. 8. The volatile aluminum chloride product was drawn into an off-gas trap, where it condensed and was collected. The salt blend in the glassy carbon crucible was then heated to 700°C at 5°C/min, the cover was removed, and the salt was stirred momentarily with a glassy carbon rod to assure homogeneity. The furnace was de-energized and the crucible was allowed to cool to ambient temperature. The salt ingot was removed from the glassy carbon crucible and crushed, from which random grab samples (referred to as bottoms) were taken for analysis. The off-gas trap was opened, and random grab samples (referred to as distillates) were taken for analysis.

The second run was a repeat of the first run, with the exception that a nominal 5 g of aluminum foil in 1 cm × 1 cm pieces was added to the blend along with an additional 33 g of ammonium chloride. The third and fourth runs mirrored the first two runs, with the exception that the chloride feed materials were exchanged for bromide feed materials and heating was limited to 650°C.

The crushed bottoms product from the first run was re-blended with additional ammonium chloride particulate and subjected to the same heating and sampling operations as the previous runs to assess the impact of additional excess ammonium chloride on the process. The same approach was applied to crushed bottoms product from the third run with additional excess ammonium bromide. Samples from each of these two repeat runs were subjected to the same analyses as the previous four runs.

A portion of the distillate product from Run 2 was blended with magnesia powder and sodium chloride particulate and heated to 800°C to investigate a technique to process an aluminum chloride distillation product into a waste form as part of this series of experiments. A

10% stoichiometric excess of magnesia powder was added to react with the Run 2 distillate product, which was assumed to be pure aluminum chloride, per the reaction mechanism below. [10]

$$3\ MgO + 2\ AlCl_3 \rightarrow Al_2O_3 + 3\ MgCl_2 \qquad \Delta G_{f,800C} = -311.976\ kJ/mol \qquad (9)$$

Sufficient sodium chloride was preloaded in the blend to form a eutectic mixture of sodium chloride with the produced magnesium chloride (i.e., NaCl – 41.5 mol% $MgCl_2$ with a binary eutectic melting point of 445°C). [23] After cooling to an ambient temperature, the consolidated product was crushed, and a random sample was taken for analysis. A summary of conditions for the series of experiments is shown in Table 1.

Equipment

The primary pieces of equipment for the series of halogenation and waste-form runs included a furnace and an off-gas trap assembly. A bench-top jeweler furnace (Kerr, Auto Electro-Melt Furnace, Maxi 3kg) was used to heat the mixtures of salts and metals. The furnace instrumentation was modified to facilitate ramp rate and cut-out temperature controls. The vendor-provided graphite crucible within the furnace was machined to accommodate a tapered glassy carbon crucible (SIGRADUR, GAT 32, 320 ml). The glassy carbon crucible was covered with an off-gas trap assembly that stood adjacent to the furnace. The off-gas trap assembly consisted of a 160-mm diameter by 220-mm-tall stainless-steel can with a sealed removeable upper flanged lid that was fitted with a 50-mm-diameter inlet line and a 6-mm-diameter outlet line. The can was configured with a set of stainless-steel heat shields that stood 50 mm off the bottom and 50 mm below the top of the can. The heat shields had a 55-mm-diameter open center to accommodate a 50-mm-diameter downcomer inlet tube that was fixed to the lid. The annulus

between the heat shield and the downcomer tube, as well as the annulus between the heat shields and the can, were packed with steel wool to trap distillate product in the bottom of the can. The inlet line was fitted with two 90-degree elbow joints, the outer of which was fitted with a bell cap that flared to a 75-mm diameter scalloped open end, covering the top open end of the glassy carbon crucible in the furnace. The furnace and off-gas trap assembly were configured on a bench-top inside an argon atmosphere glovebox (MBRAUN LABmaster dp). The trap outlet was fitted with a flexible gas line that passed through a filter (MotorGuard, 0.01-micron filter element) and rotameter (Brooks Instrument) inside the glovebox, through the glovebox wall, and to a vacuum pump (Gast Manufacturing, model DOA-P704-AA) outside the glovebox. The off-gas system facilitated a sweep gas across the open glassy carbon crucible to quench and direct volatile species into the off-gas trap. Pictures of the furnace and off-gas trap assembly are shown in Figure 3. A simplified sectional view of the furnace and off-gas trap assembly is illustrated in Figure 4.

Materials

The primary materials for the series of halogenation and waste-form runs consisted of reactive ammonium salts, reactive metals, diluent salts, and a neutralizing oxide. Ammonium chloride and ammonium bromide are hygroscopic materials and were not available in a high-purity anhydrous form from suppliers. Consequently, the ammonium chloride (Alfa Aesar, 99.999%, Puratronic) and ammonium bromide (Alfa Aesar, 99.999%, Puratronic) used in this study were dried, crushed, and sieved to the desired particle size using a bench-top box furnace in an argon atmosphere glovebox. Specifically, the procured granular ammonium salts were loaded into trays and heated to 120°C for at least 20 hours, followed by heating at 140°C for at least four hours. The dried material was crushed and sieved to particle sizes below 30 mesh.

The reactive metals included neodymium metal powder (Alfa Aesar, 99.9%), aluminum metal powder (Alfa Aesar, 99.97%), and aluminum foil (Alfa Aesar, 99.99%, 0.25-mm thick). The metal powders are pyrophoric materials and were handled under an argon atmosphere. The neodymium metal powder was procured in nominal 5 g packages, each of which was used in its entirety in a halogenation run. The thickness of the aluminum foil added to the mixtures of Run 2 and 4 approximated that of used ATR cladding.

Diluent salts included lithium chloride (Alfa Aesar, 99.9%, ultra-dry), lithium bromide (Alfa Aesar, 99.97%, ultra-dry), and sodium chloride (Sigma Aldrich, 99.999%), each of which was procured as anhydrous 10-mesh beads packaged under argon. Each of these alkali-metal chlorides was crushed and sieved to particle sizes below 30-mesh. Magnesium oxide (J. T. Baker, powder) was used as a neutralizing oxide for the aluminum chloride distillate product from Run 5 to produce, along with sodium chloride, a consolidated waste form.

Sample Characterization

Product samples from the series of halogenation and waste-form runs were halved, forming two sample sets for chemical and diffraction analyses. One set of product samples was characterized for elemental composition via inductively coupled plasma – optical emission spectroscopy (ICP-OES). The solid samples were dissolved in 2% nitric acid and then diluted prior to ICP-OES analysis. The other set of samples were ground into fine powders and characterized using X-ray diffraction (XRD) (Rigaku SmartLab, Cu Kα, 40 kV and 44 mA). The XRD data were collected between 10 – 80° with a step of 0.04° at 4° per minute.

Calculations

The high surface area of neodymium and aluminum metal powder feed materials along with the multiple constituent phases that were expected in this series of runs created a complex set of conditions that warranted calculations prior to proceeding with the experiments. Specifically, a model was created to assess possible chemical equilibrium conditions and related reaction mechanisms to ensure that intended products under the design operating conditions would likely be formed. Chemical equilibrium calculations provide a straightforward means of assessing product compositions as a function of temperature for a given quantity of raw materials. Commercially available software [10] was used to perform such calculations with a Gibbs energy minimization model, which is based on prior work by others. [24] After inputting the defined feed materials for Run 1 (i.e., 5 g of neodymium metal, 5 g of aluminum metal, 50 g of lithium chloride and 38.8 g of ammonium chloride) and assuming unit activities and ideal mixing, the model produced a plot of possible constituent equilibrium inventories as a function of temperature, as shown in Figure 5. Only the predominant compounds of the 47 selected possible compounds are shown in Figure 5. A noteworthy finding from the model for Run 1 is the decomposition of ammonia into nitrogen and hydrogen gases from possible intermediate interactions with neodymium and aluminum. Indeed, the model identifies the formation and enduring presence of aluminum nitride, which would preclude its separation from neodymium. Another finding from the model is the intermediate formation of lithium-aluminum chloride, which decomposes into lithium chloride and gaseous aluminum chloride at temperatures above the normal sublimination point (i.e., 180°C) of aluminum chloride.

A similar model was created for Run 3, which produced a nearly identical outcome except for the presence of bromide compounds in lieu of the companion chloride compounds. Another model was generated for Run 5 with input masses of 30 g of aluminum chloride, 3.6 g

of ammonium chloride, 15 g of magnesium oxide, and 28 g of sodium chloride. The model produced a plot of possible constituent concentrations as a function of temperature, as shown in Figure 6. For modeling purposes, it was assumed that the 10% excess ammonium chloride from Run 2 resided with the aluminum chloride distillate.

The primary finding from the model of Run 5 is the conversion of magnesium oxide and aluminum chloride to aluminum oxide and magnesium chloride, the latter of which leads to a variety of mixed chloride compounds with sodium chloride. The model also shows excess magnesium oxide forming mixed magnesium and aluminum oxides. Excess ammonium chloride appears to be inconsequential in this model, as it decomposes into nitrogen, hydrogen, and hydrogen chloride gases.

Results

In the first run, we blended 5.081 g of neodymium metal powder, 5.023 g of aluminum metal powder, 39.084 g of ammonium chloride particulate, and 50.042 g of lithium chloride particulate in a 250-ml glass jar, as shown in Figure 7. The mixture was transferred to a pre-weighed glassy carbon crucible, also shown in Figure 7. After heating the mixture to 700°C and removing the off-gas trap from atop the glassy carbon crucible, the molten solution was stirred with a glassy carbon rod and no solid phase was apparent. The furnace was de-energized, and the cooled salt ingot separated readily from the glassy carbon crucible. The ingot was halved, revealing an upper dark layer and lower light layer, as shown in Figure 8. The off-gas trap was opened, revealing a loose fine colorless powder, as shown in Figure 8.

The procedure was repeated for Runs 2–4, as outlined in Table 1. A picture of the loose blend of materials for Run 2, including aluminum metal foil pieces, is also shown in Figure 7. The bottoms and distillate products for Runs 2–4 exhibited similar colors and consistencies to

those from the first run. No degradation or change in mass was observed in the glassy carbon crucible throughout the series of runs. Notable mass measurements for the halogenation runs are listed in Table 2.

In the fifth run, we blended 30.000 g of the distillate product from Run 2 with 14.963 g of magnesium oxide and 27.804 g of sodium chloride in a glass jar, of which 72.728 g was transferred to a glassy carbon crucible and heated as outlined in Table 1. At 800°C, the off-gas trap was removed, and there was no visible collection of any off-gas particulate. The molten solution was stirred with a glassy carbon rod, exhibiting an off-white opaque slurry consistency. The furnace was de-energized, and the cooled ingot separated readily from the glassy carbon crucible. The mass of the bottoms product was 62.527 g. The ingot was broken, revealing an off-white consistency throughout, as shown in Figure 9 along with the blend before and after consolidation. The bottoms product was crushed, and a random grab sample was taken for XRD analysis.

Each of the bottoms and distillate product samples was subjected to elemental analysis for neodymium, aluminum, and lithium via ICP-OES, the results of which, with a margin of error of ± 5–15% at 2 sigma, are shown in Table 3.

The bottoms and distillation samples from Runs 1–5 were ground to a powder, from which XRD sample trays were prepared and analyzed. The XRD patterns for the samples of chloride bottoms products (Runs 1, 1.1, and 2) were similar, revealing in order of prevalence LiCl and $NdCl_3$ in all three runs and possibly Nd in Run 2. The XRD patterns for bottoms products from Runs 1, 1.1, and 2 are shown in Figure 10.

The XRD patterns for the samples of bromide bottoms products (Runs 3, 3.1, and 4) were similar, revealing in order of prevalence LiBr and $NdBr_3$ for each of these runs. The XRD patterns for bottoms products from Runs 3, 3.1, and 4 are shown in Figure 11.

The XRD patterns for chloride distillate products from Runs 1 and 2 were similar, each revealing in order of prevalence NH_4Cl and $(Al(NH_3)_4Cl_2)(AlCl_4)$, while NH_4AlCl_4 was an additional compound identified in Run 1. The XRD pattern for Run 1.1 only revealed the presence of NH_4Cl. The XRD patterns for distillate products from Runs 1, 1.1, and 2 are shown in Figure 12.

The XRD patterns for bromide distillate products from Runs 3 and 4 were similar, each revealing in order of prevalence NH_4Br and $(AlBr_3)(NH_3)_5$. The XRD pattern for Run 3.1 only revealed the presence of NH_4Br. The XRD patterns for distillate products from Runs 3, 3.1, and 4 are shown in Figure 13.

As a multicomponent material, the XRD patterns for the waste-form product from Run 5 identified a variety of compounds, including mixed sodium-magnesium chloride, sodium chloride, magnesium aluminate, magnesia, and possibly a mixed sodium-aluminum chloride. The XRD pattern for the product from Run 5 is shown in Figure 14.

Discussion

The series of halogenation and waste-form runs demonstrated specific dissolution and separation techniques using non-radiological materials and simplified approaches to address the following primary issues, which included (1) the extents of aluminum and neodymium separation as a function of metal feed forms (i.e., powder versus foil) and halogenating agents (chloride versus bromide) and (2) how to stabilize the generated aluminum halide distillate

product. Another issue is how the techniques in this demonstration might apply to used ATR fuel.

The performance of this series of halogenation runs was consistent with the identified reaction mechanism in Eq. 8, as evidenced by material balances and characterized product compositions. The theoretical compositions of reaction products per Eq. 8 for the series of halogenation runs were calculated based on feed material inputs and the following assumptions. First, the prescribed blends of metal powders, aluminum foil, ammonium halide, and lithium halide in a new glass jar each run did not completely transfer to the glassy carbon crucible in all cases, as some residual powder adhered to the inner jar walls. We assumed that the mixtures that were transferred to the glassy carbon crucible for each run contained the same proportions of materials that were initially loaded into the respective glass jars. Second, all the nitrogen and hydrogen from the ammonium halides, as well as any excess ammonium halide, separated from the bottoms as an off gas. Third, all the neodymium metal was converted to its respective halide upon reaction with ammonium halide and fused with its respective lithium halide. Fourth, all the aluminum metal was converted to its respective halide upon reaction with ammonium halide and volatilized away from the fused salt phase. Finally, the ammonium halide in contact with the crushed bottoms products of Runs 1.1 and 3.1 volatilized away from the fused salt and collected in the off-gas trap, leaving the mass of the bottoms unchanged. Accordingly, the calculated masses of the bottoms for each of the halogenation runs are compared with their respective measured masses from Table 2 for comparison in Table 4.

A 99.3% ratio of measured to calculated mass of bottoms in Run 1 suggests that essentially all the aluminum in the mixture reacted and separated from the bottoms, which is consistent with product characterization analyses. Specifically, the aluminum in the bottoms

fraction was below detection levels, and no lithium or neodymium was detected in the distillate fraction. Proportioning the mass of loaded aluminum in this run to that of neodymium correlates to an aluminum removal of >97%. The XRD analysis of the distillate product for this run identified the presence of aluminum chloride, in combination with ammonia and excess ammonium chloride in the forms of $(Al(NH_3)_4Cl_2)(AlCl_4)$ and NH_4AlCl_4, respectively. Additionally, a separate phase of excess ammonium chloride was identified in the distillate product.

In Run 1.1, the bottoms mass was little changed from the loaded crushed product, suggesting that essentially all the aluminum metal from this batch had reacted and volatilized away from the bottoms in the first run. However, a larger sample size of the bottoms revealed a detectable fraction of aluminum, correlating to a 98.2% removal. The fact that additional excess ammonium chloride did little if anything to remove aluminum metal suggests that the aluminum in the bottoms fraction was no longer in a metallic state. The absence of aluminum chloride and the sole presence of ammonium chloride in the XRD analysis of the distillate fraction corroborates the absence of aluminum metal in the bottoms.

In Run 2, a 101.1% ratio of measured-to-calculated mass in the bottoms suggests that a 10% excess of ammonium chloride was insufficient to react with all the aluminum metal, which is likely due to the addition of the aluminum foil. The aluminum content in the bottoms equated to a 94.5% extent of aluminum removal, while no lithium or neodymium was detected in the distillate fraction. Like Run 1, the XRD analysis of the distillate product for Run 2 identified the presence of aluminum chloride in combination with ammonia and excess ammonium chloride.

The bromination runs 3, 3.1, and 4 produced similar results to those of the corresponding chlorination runs. More than 95% of the aluminum metal was removed from the loaded salt-

metal blend in Run 3, based on minimum detection levels of aluminum in the bottoms. Exposure of the bottoms from Run 3 to additional excess ammonium bromide in Run 3.1 yielded a detectable fraction of aluminum via ICP-OES in the distillate, even though only ammonium bromide was detected in the distillate via XRD. Aluminum at 1,490 ppm was detected in the bottoms fraction of Run 3.1, which equated to a 97.8% removal. This extent of removal was nearly identical to that of the corresponding chlorination run despite the additional loading of ammonium bromide, again suggesting that the remaining aluminum in the bottoms fraction was nonmetallic. The extent of aluminum removal in Run 4 was 91.4%, underscoring the more challenging removal of aluminum in a foil form as opposed to powder.

In bromination runs 3, 3.1, and 4, no lithium or neodymium was detected in the distillate fraction via ICP-OES or XRD. Ammonium bromide was identified in each of the distillate fractions, while aluminum bromide in combination with ammonia was the primary compound in the distillate fractions for Runs 3 and 4.

In short, halogenation runs 1–4, with their accompanying repeat runs, proceeded in accordance with the reaction mechanism identified in Eq. 8 with varying extents of aluminum removal. No lithium or neodymium halides were detected in any of the distillate products. The identification of ammonia compounds with aluminum chloride and bromide distillates in Runs 1–4 suggests that ammonia did not appreciably decompose into nitrogen and hydrogen gases, as suggested by the equilibrium models (see Figure 5). Excess ammonium halides were identified in all the distillate products, showing how their sublimed decomposition products (i.e., hydrogen halide and ammonia gases) recombined in the off-gas system.

The fine, low bulk density particulate form of the distillate products is not a preferable form for direct disposal. Consequently, a separate Run 5 was performed with the aluminum

chloride distillate from Run 2 to demonstrate a preferable waste form. The run proceeded largely in accordance with the reaction mechanism identified in Eq. 9 and the equilibrium model from Figure 6. Specifically, magnesium oxide reacted with aluminum chloride to form stable magnesium aluminate, a compound of magnesia and alumina, and magnesium chloride. The magnesium chloride formed stable mixed chlorides with the loaded sodium chloride. The product also contained excess sodium chloride, magnesium oxide, and possibly sodium-aluminum chloride. In short, Run 5 demonstrated the conversion of a mobile, low bulk density aluminum chloride bearing powder into an immobilized, consolidated, solid waste-form suitable for disposal.

Regarding extension of this halogenation technique to used ATR fuel, the simplifying portions of this study need to be addressed. First, ammonium halides were used out of convenience in this study to deliver a hydrogen halide gas to the reactive metals without installing a dedicated gaseous hydrogen halide system. In the halogenation of used ATR fuel, a gaseous halogenation system would be preferable. As such, ammonia gas would not be present in the off-gas system, as it was in this study. Second, neodymium metal was used in this study as a surrogate for uranium metal. Neodymium forms intermetallics with aluminum (e.g., $NdAl_2$), as does uranium. However, no prepared neodymium and aluminum intermetallics were used in this study because they were expected to halogenate completely, as was observed in previous work with uranium and aluminum intermetallics [17-20] and as shown in the following chlorination reaction. [10]

$$NdAl_2 + 9\ NH_4Cl \rightarrow NdCl_3 + 2\ AlCl_3 + 9\ NH_3(g) + 4.5\ H_2(g), \quad \Delta G_{f,500C} = -1192\ kJ/mol \qquad (10)$$

Another factor in the use of neodymium metal as a surrogate for uranium metal is that neodymium halide formation is limited to the trivalent state, while uranium exhibits tetra-, penta-, and hexavalent chlorides. Thus, chlorination of a uranium and aluminum matrix would need to account for the higher vapor pressures associated with the higher valence states of uranium chloride in regard to its separation from aluminum chloride. In contrast, uranium in a bromide system would be largely limited to the tetrabromide, as uranium pentabromide decomposes to the tetrabromide and elemental bromine above 80°C. [25] Thus, the bromination of used ATR fuel could be less likely to exhibit volatile uranium species than those from a chlorination system. However, hydrochlorination or hydrobromination of a uranium and aluminum matrix would limit the valence states of uranium to the respective tri- and tetrahalide due to the presence of hydrogen in the gas phase (see Eq 6).

Another significant factor to consider in regard to extension of this halogenation technique to used ATR fuel is the effect on fission products, which would introduce a wide variety of possible halide formations and accompanying volatilities. However, investigation into the fate of fission products for the subject halogenation technique is beyond the scope of this work.

Conclusions

We performed a series of experiments with surrogate materials at bench scale, which successfully demonstrated and characterized a halogenation technique applicable to the treatment of used aluminum matrix test reactor fuel. The demonstration utilized neodymium metal as a non-radiological surrogate for uranium metal, along with aluminum metal powder and aluminum foil as the primary constituents of an aluminum matrix fuel. Ammonium chloride and bromide were effective at dissolving the metal matrix, causing the respective aluminum halide to gasify

and separate from the formed neodymium halide, which then fused with its corresponding lithium halide as a nonreactive diluent. Specifically, a 10% stoichiometric excess of ammonium chloride removed more than 97% of the aluminum metal in powder form, while the same removed 94.5% of the aluminum metal in a combined form of powder and foil. Similarly, ammonium bromide removed more than 95% of the aluminum metal in powder form, while the same removed 91.4% of the aluminum metal in a combined form of powder and foil. Additions of ammonium halide beyond the 10% stoichiometric value in repeat runs pushed the extents of aluminum removal to 98.2% and 97.8% for the chlorinating and brominating systems, respectively. No neodymium or lithium halides were detected in the off-gas products, which were limited to compounds of aluminum halide, ammonia, and excess ammonium halide. A separate experiment was performed with off-gas product from one of the chlorination runs, which successfully reacted and consolidated the fine, low bulk density material with magnesia and sodium chloride into a solid matrix of magnesium-aluminum oxides and sodium-magnesium chlorides. This study identified a viable technique for use with aluminum matrix test reactor fuels, including used ATR fuel. A demonstration of this technique with an unirradiated aluminum matrix fuel to address the fate of uranium halides would be a logical next step.

Acknowledgements

This work was supported through the INL Laboratory Directed Research & Development (LDRD) Program under DOE Idaho Operations Office Contract DE-AC07-05ID14517.

References

[1] Glagolenko I, Wachs D, Woolstenhulme N, Chang G, Rabin B, Clark C. Irradiation testing of the RERTR fuel miniplates with burnable absorbers in the advanced test reactor. Proceedings of RERTR 2010; 2010 Oct 10–14; Lisbon, Portugal.

[2] Petersen G. Evaluation of Neutron Absorbers in the DOE Standardized SNF Canister. Idaho Falls (ID): Idaho National Laboratory; 2019. (INL/EXT-19-53193).

[3] Stahl D. Fuels for Research and Test Reactors, Status Review: July 1982. Lemont (IL): Argonne National Laboratory; 1982. (ANL-83-5).

[4] Research Reactor Core Conversion Guidebook, Volume 4: Fuels (Appendices I-K). Vienna (Austria): International Atomic Energy Agency; 1992. (IAEA-TECDOC-643).

[5] Lundberg LB and Croson ML. Corrosion of Spent Advanced Test Reactor Fuel. Idaho Falls (ID): Idaho National Engineering and Environmental Laboratory; 1994. (EGG-M-9422).

[6] US Nuclear Waste Technical Review Board. Management and Disposal of U.S. Department of Energy Spent Nuclear Fuel -- A Report to the United States Congress and the Secretary of Energy. Arlington (VA); 2017.

[7] US Department of Energy. Record of Decision for the Treatment and Management of Sodium-Bonded Spent Nuclear Fuel. Federal Register. 2000;65(182):56565–56570.

[8] Final Environmental Impact Statement for the Treatment and Management of Sodium-Bonded Spent Nuclear Fuel. Washington DC: US Department of Energy; 2000. (DOE/EIS-0306).

[9] National Research Council. Electrometallurgical techniques for DOE spent fuel treatment: final report (2000). Washington DC: National Academy Press; 2000. ISBN 978-0-309-07095-9.

[10] Outotec, HSC Chemistry 8, Pori (2015).

[11] ASM International, Diagram No. 900138 (2006).

[12] Herrmann S, Norbash K, Wachs D. Fray International Symposium, Volume 3: Molten Salts and Ionic Liquids. Quebec (Canada): FLOGEN STARS OUTREACH; 2012. Separation and recovery of uranium from next generation research reactor fuel via molten salt electrorefining; p. 151–164. ISBN: 978-0-9879974-0-1.

[13] Willit JL, Gay EC, Miller WE, McPheeters CC, and Laidler JJ. Electrometallurgical treatment of aluminum-matrix fuels. Proceedings of the DOE Spent Nuclear Fuel and Fissile Material Management Embedded Topical Meeting; 1996 June 16–20; Reno, NV.

[14] McPheeters CC, Gay EC, Karell EJ, and Ackerman JP. Electrometallurgically treating metal, oxide, and al alloy spent nuclear fuel types. JOM. 1997;49:22–25.

[15] Willit JL, Slater SA, Raraz A, and Gay EC. Electrometallurgical treatment of aluminum-based fuels. Proceedings of the Third Topical Meeting on DOE Spent Nuclear Fuel and Fissile Materials Management; 1998 Sept 8–11; Charleston, SC.

[16] Slater SA, Raraz AG, Willit JL, Gay EC. Electrochemical separation of aluminum from uranium for research reactor spent nuclear fuel applications. Sep Purif Technol. 1999;15(3):197–205.

[17] Mendes E, Cassayre L, Malmeck R, Soucek P, Jardin R, Glatz JP. Recovery of actinides from actinide-aluminum alloys: chlorination route. Proceedings of the ATALANTE 2008; 2008 May 19–22; Montpellier (France).

[18] Soucek P, Malmbeck R, Mendes E, Nourry C, Jardin R, Glatz JP. Separation of uranium from uranium-aluminum alloys by chlorination process. Proceedings of Global 2009; 2009; Paris (France).

[19] Soucek P, Malmbeck R, Nourry C, and Glatz JP. Pyrochemical reprocessing of spent fuel by electrochemical techniques using solid aluminum cathodes. Energy Procedia. 2011;7:396–404.

[20] Meier R, Soucek P, Malmbeck R, Fanghaenel T. Recycling of uranium from uranium-aluminum alloys by chlorination with HCl(g). Procedia Chemistry. 2012;7:785–790.

[21] Rumble JR, Ed. *CRC Handbook of Chemistry and Physics* (102nd ed.). CRC Press/Taylor & Francis; Boca Raton, FL; 2021. ISBN: 9780367712600.

[22] Bohel A, Nassini H, Bevilacqua A, and Pasquevich D. Chlorination reactions applied to reprocessing of aluminum-uranium spent nuclear fuels. Mater Res Soc Symp Proc. 1997;506:535.

[23] Grjotheim K, Holm JL, Roetnes M. System $MgCl_2$ – NaCl. (1972) Phase Equilibrium Diagram No. 5661 in *ACerS – NIST Phase Equilibria Diagrams*, National Institute of Standards and Technology, PC Database, Version 4.0, Gaithersburg, Maryland (2013).

[24] White WB, Johnson SM, Dantzig GB. Chemical equilibrium in complex mixtures. J Chem Phys. 1958;28:751.

[25] Blair A and Ihle H. The thermal decomposition and thermodynamic properties of uranium pentabromide. J Inorg Nucl Chem. 1973;35:3795.

Table 1. Conditions for series of halogenation and waste-form runs.

Run	Mixture Components	Heating Cycle	Samples
1	LiCl particulate, Nd metal powder, Al metal powder, NH_4Cl particulate	Ambient → 500°C at 10°C/hr 500 → 700°C at 5°C/min	Crushed bottoms, distillate product
1.1	Crushed Run 1 bottoms, additional NH_4Cl particulate		Crushed bottoms, distillate product
2	LiCl particulate, Nd metal powder, Al metal powder, Al foil, NH_4Cl particulate		Crushed bottoms, distillate product
3	LiBr particulate, Nd metal powder, Al metal powder, NH_4Br particulate	Ambient → 500°C at 10°C/hr 500°C → 650°C at 5°C/min	Crushed bottoms, distillate product
3.1	Crushed Run 3 bottoms, additional NH_4Br particulate		Crushed bottoms, distillate product
4	LiBr particulate, Nd metal powder, Al metal powder, Al foil, NH_4Br particulate		Crushed bottoms, distillate product
5	Run 2 distillate, MgO powder, NaCl particulate	Ambient → 500°C at 10°C/hr 500°C → 800°C at 5°C/min	Crushed consolidated product

Table 2. Summary of recorded masses from halogenation Runs 1–4.

Grams \ Run	1	1.1	2	3	3.1	4
Pre-run masses in glass jar						
Nd powder	5.081	—	5.005	5.116	—	5.000
Al powder	5.023	—	5.171	5.086	—	5.144
Al foil	—	—	5.002	—	—	5.086
NH_4Cl	39.084	16.116	72.682	—	—	—
NH_4Br	—	—	—	72.389	15.695	133.749
LiCl	50.042	—	50.012	—	—	—
LiBr	—	—	—	50.202	—	50.314
Crushed bottoms	—	54.593	—	—	59.318	—
Pre-run masses in crucible						
Total loose blend	99.233	70.709	137.894	132.746	74.970	199.300
Post-run product mass in crucible						
Bottoms	58.418	54.526	59.377	63.427	59.069	65.262

Table 3. Elemental analysis results for bottoms and distillate samples from Runs 1–4.

ppm \ Run	1	1.1	2	3	3.1	4
Distillate						
Al	124,000	<1,100	125,000	74,400	5,730	61,900
Li	<330	<110	<280	<150	<110	<80
Nd	<5,300	<1800	<4,400	<2,300	<1,800	<1,300
Bottoms						
Al	<1,900	1,470	8,790	<2,500	1,490	12,600
Li	147,000	155,000	137,000	62,600	64,800	63,900
Nd	79,700	82,800	78,200	73,300	69,100	71,400

Table 4. Calculated versus measured masses of bottoms for Runs 1–4.

Grams / Run	**1**	**1.1**	**2**	**3**	**3.1**	**4**
Measured	58.418	54.526	59.377	63.427	59.069	65.262
Calculated	58.845	54.593	58.717	63.797	59.318	63.625
Meas. / Calc.	99.3%	99.9%	101.1%	99.4%	99.6%	102.6%

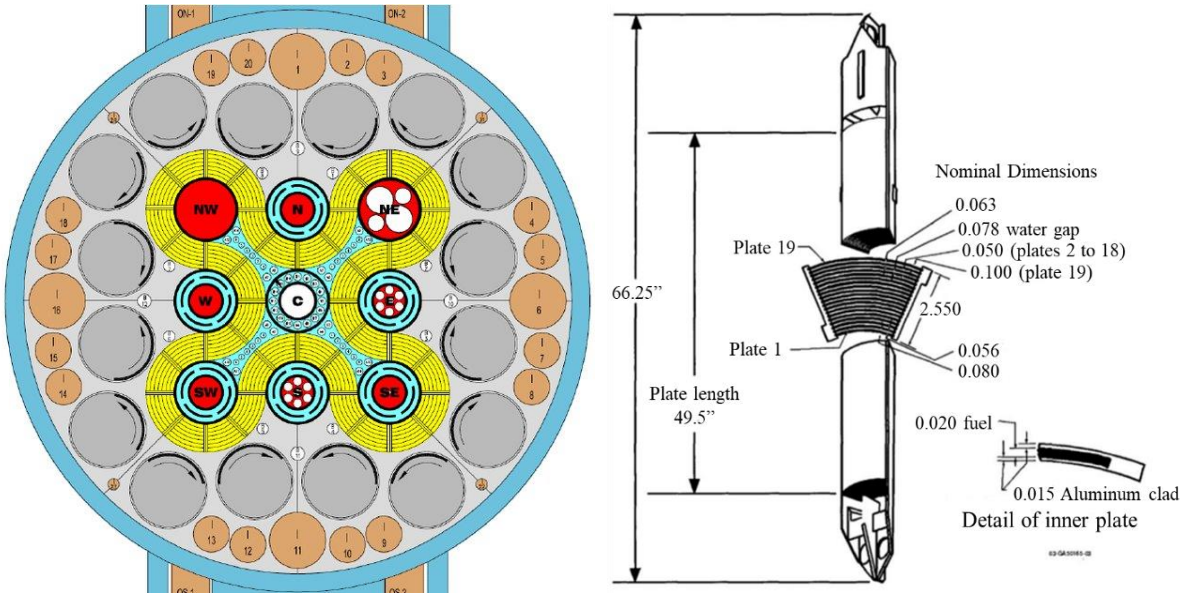
NW
N
NE
W
C
E
SW
S
SE
Nominal Dimensions
0.063
0.078 water gap
0.050 (plates 2 to 18)
0.100 (plate 19)
Plate 19
66.25”
2.550
Plate 1
0.056
0.080
Plate length
49.5”
0.020 fuel
0.015 Aluminum clad
Detail of inner plate

Figure 1.

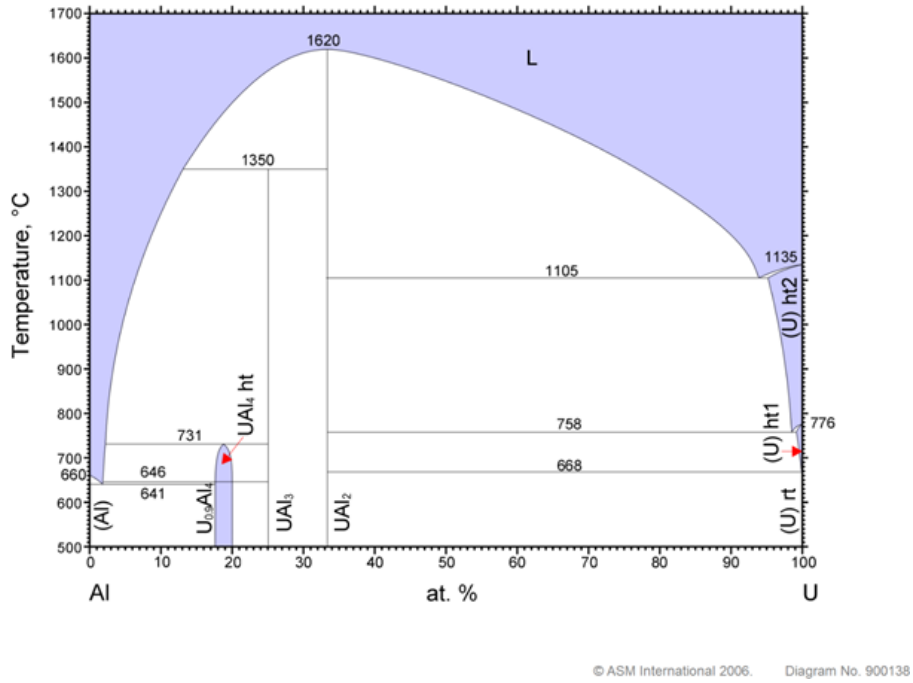
Temperature, °C
at. %
Al
U
L
1620
1350
1105
1135
(U) ht2
731
758
776
(U) ht1
646
641
668
660
(Al)
U6Al4
UAl4 ht
UAl3
UAl2
(U) rt
© ASM International 2006.
Diagram No. 900138

Figure 2.

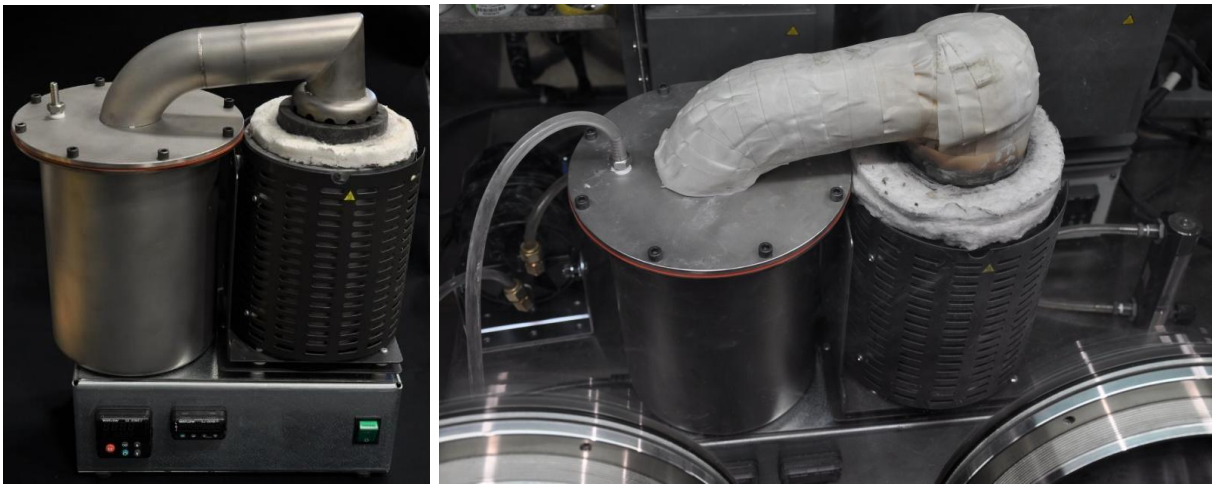

Figure 3.

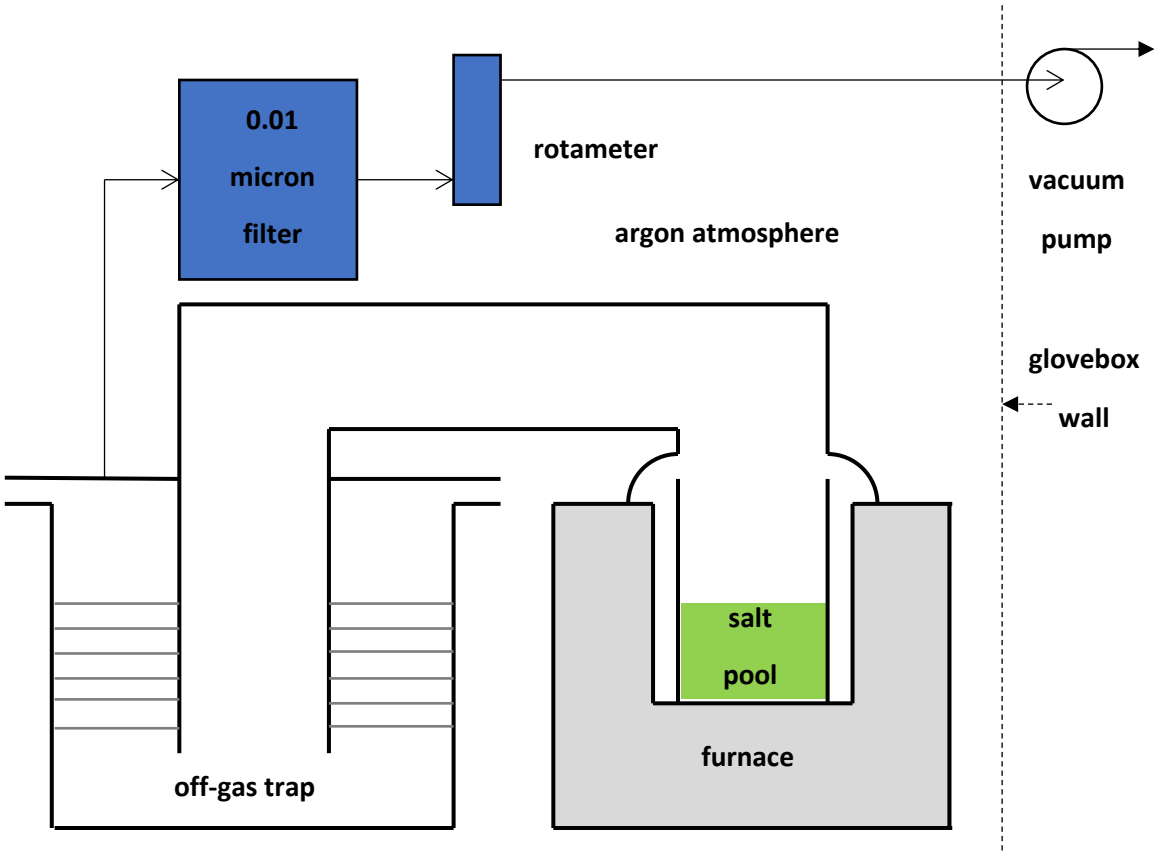
0.01
micron
filter
rotameter
vacuum
pump
argon atmosphere
glovebox
wall
salt
pool
furnace
off-gas trap

Figure 4.

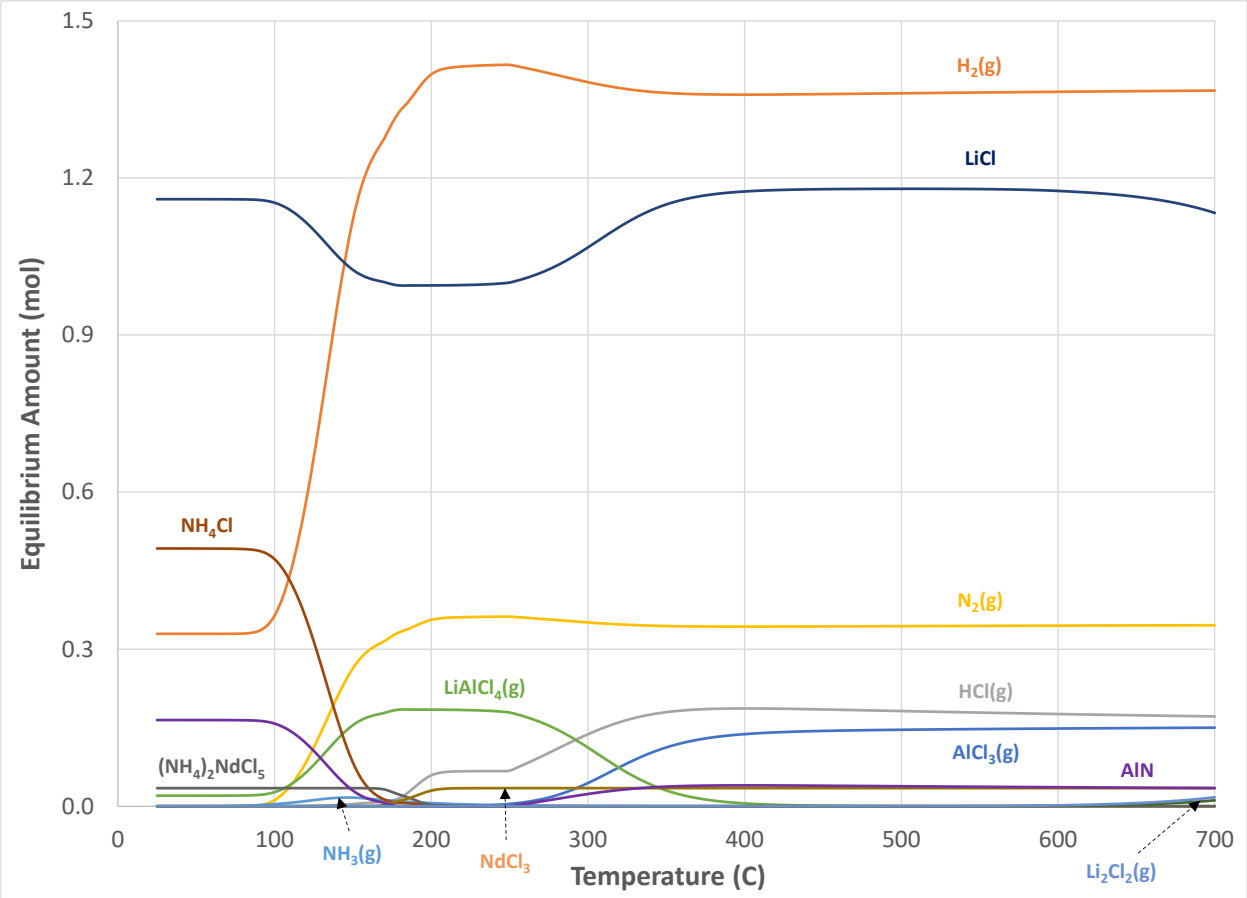
1.5
1.2
0.9
0.6
0.3
0.0
Equilibrium Amount (mol)
0
100
200
300
400
500
600
700
Temperature (C)
H2(g)
LiCl
NH4Cl
N2(g)
LiAlCl4(g)
HCl(g)
(NH4)2NdCl5
AlCl3(g)
AlN
NH3(g)
NdCl3
Li2Cl2(g)

Figure 5.

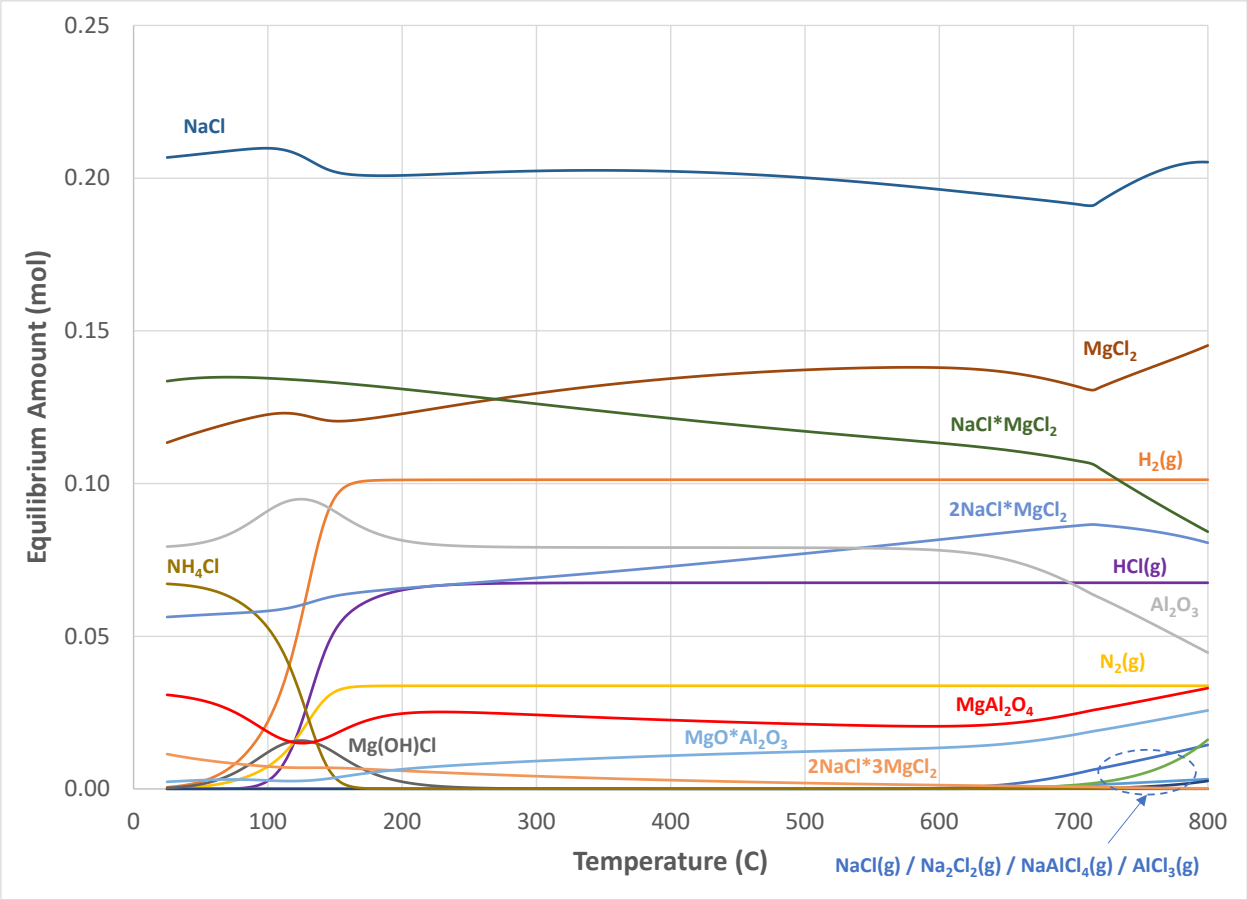
0.25
0.20
0.15
0.10
0.05
0.00
Equilibrium Amount (mol)
0
100
200
300
400
500
600
700
800
Temperature (C)
NaCl
MgCl2
NaCl*MgCl2
H2(g)
2NaCl*MgCl2
NH4Cl
HCl(g)
Al2O3
N2(g)
MgAl2O4
Mg(OH)Cl
MgO*Al2O3
2NaCl*3MgCl2
NaCl(g) / Na2Cl2(g) / NaAlCl4(g) / AlCl3(g)

Figure 6.

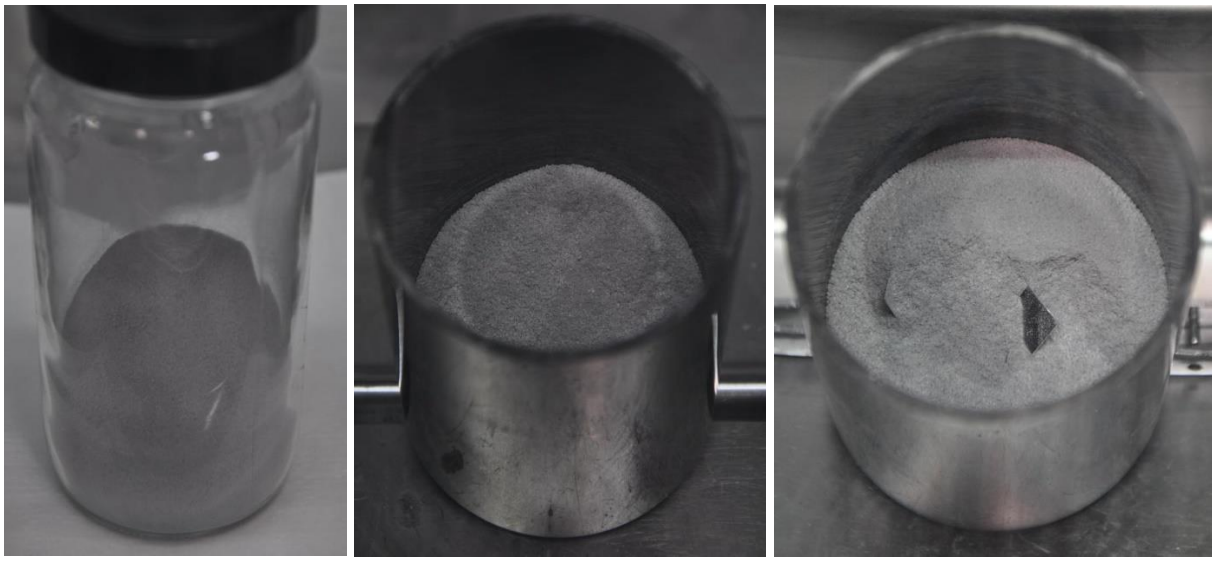

Figure 7.

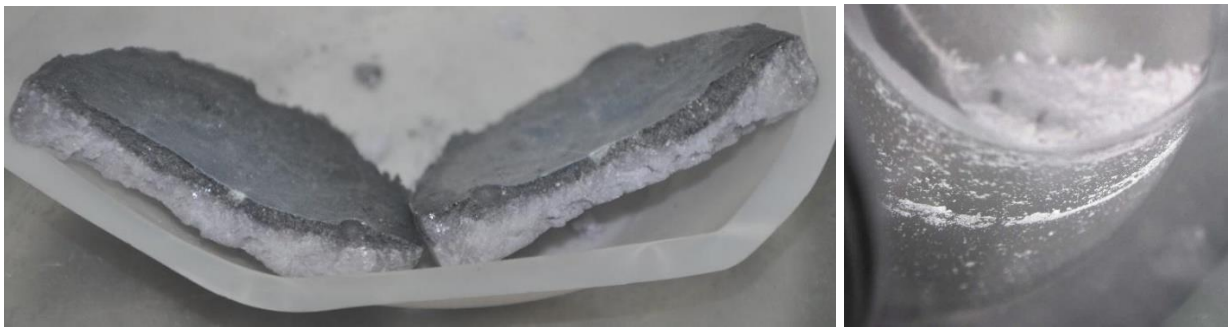

Figure 8.

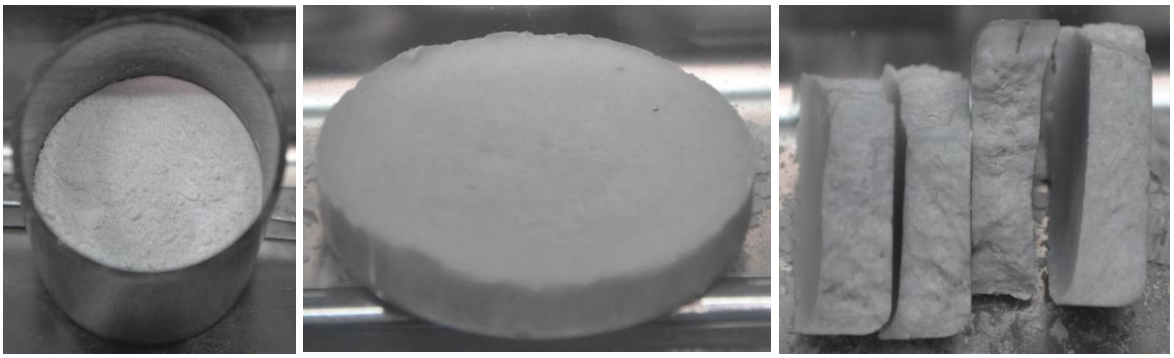

Figure 9.

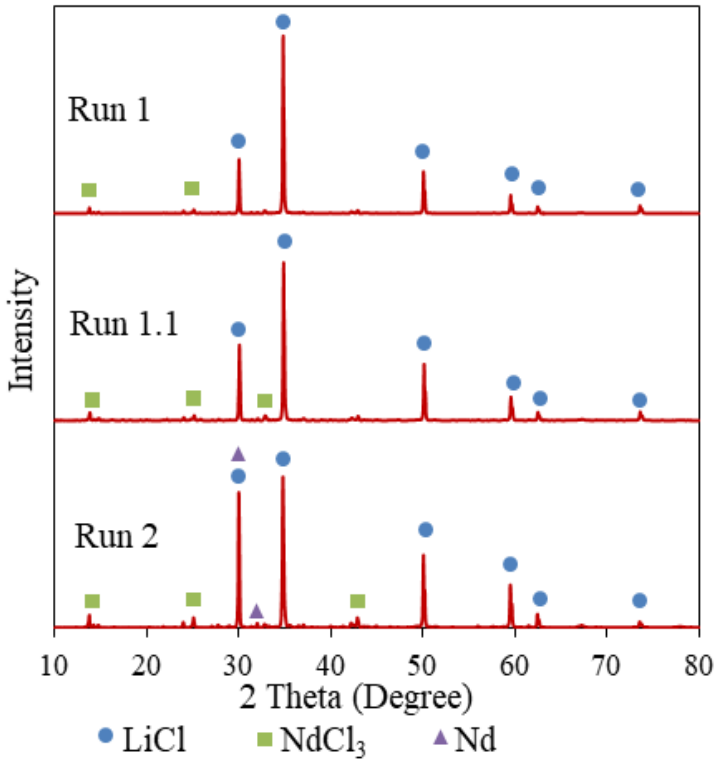
Run 1
Run 1.1
Run 2
Intensity
10
20
30
40
50
60
70
80
2 Theta (Degree)
LiCl
NdCl3
Nd

Figure 10.

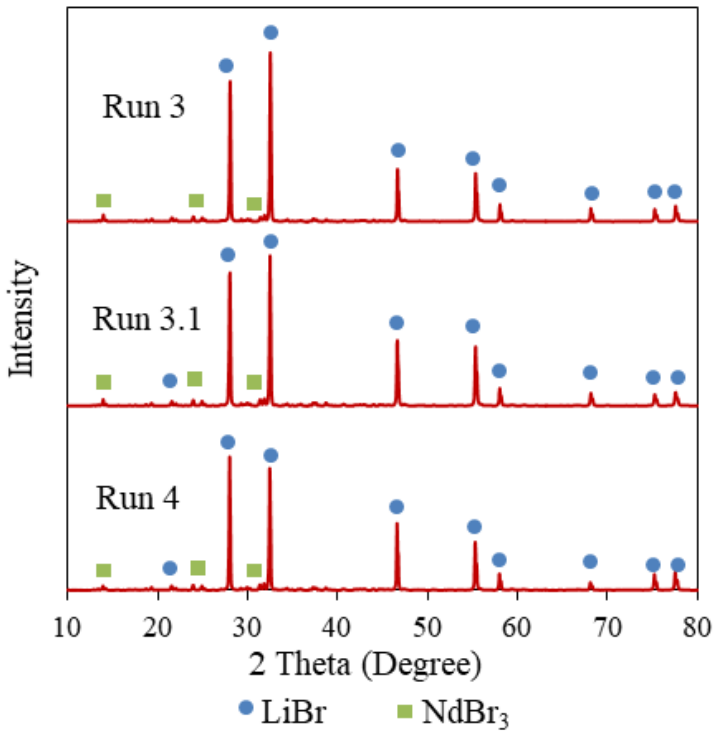
Run 3
Run 3.1
Run 4
Intensity
10
20
30
40
50
60
70
80
2 Theta (Degree)
LiBr
NdBr3

Figure 11.

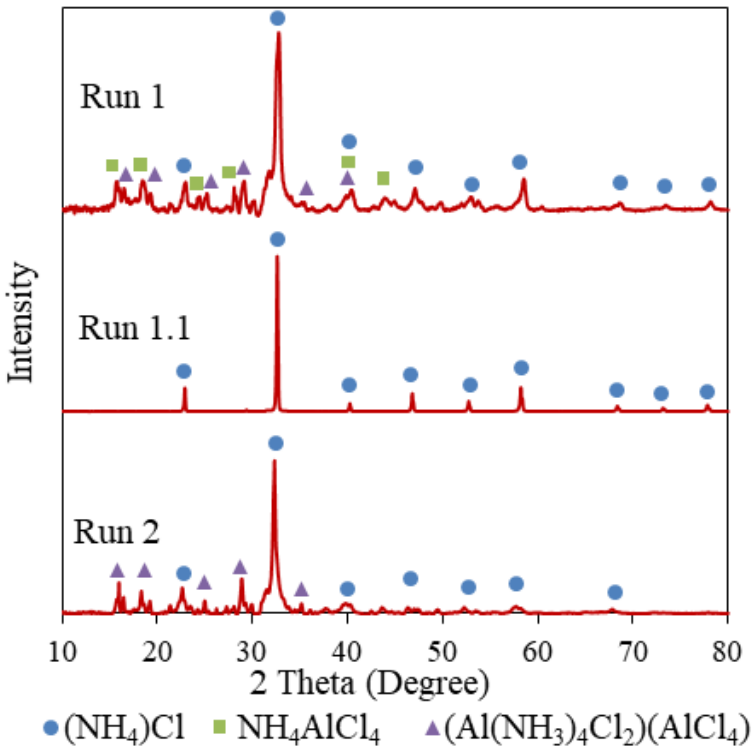
Run 1
Run 1.1
Run 2
Intensity
10
20
30
40
50
60
70
80
2 Theta (Degree)
(NH4)Cl
NH4AlCl4
(Al(NH3)4Cl2)(AlCl4)

Figure 12.

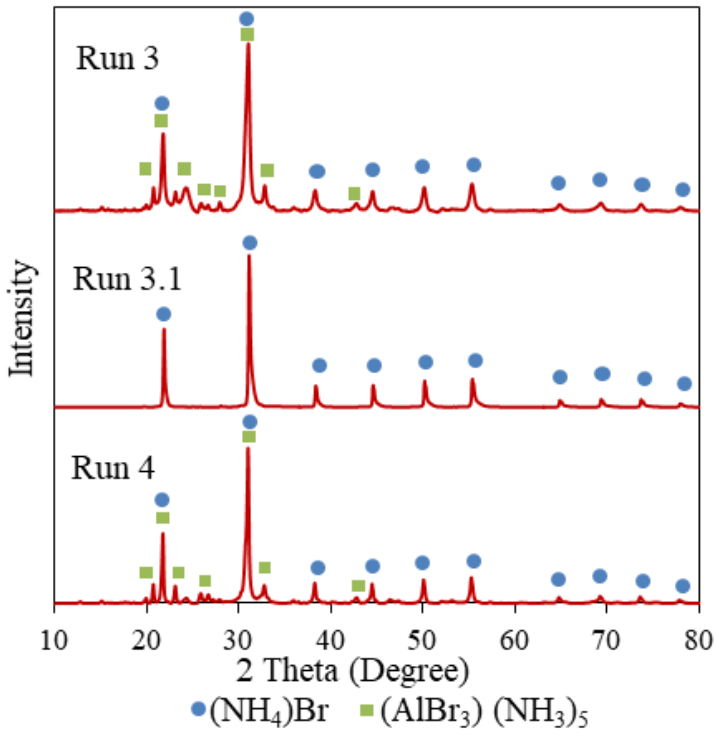
Run 3
Run 3.1
Run 4
Intensity
10
20
30
40
50
60
70
80
2 Theta (Degree)
(NH4)Br
(AlBr3) (NH3)5

Figure 13.

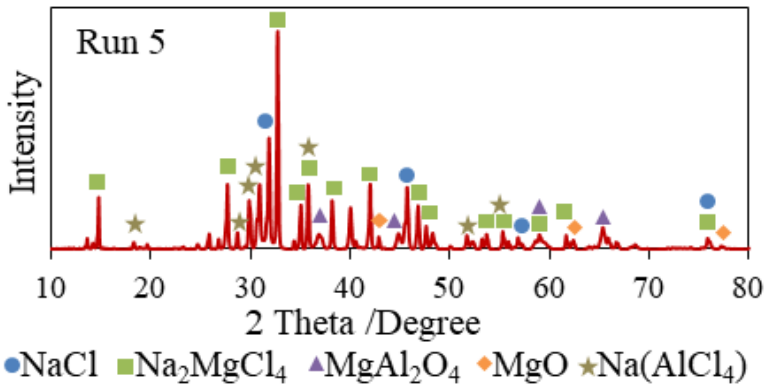
Run 5
Intensity
10
20
30
40
50
60
70
80
2 Theta /Degree
NaCl
Na2MgCl4
MgAl2O4
MgO
Na(AlCl4)

Figure 14.

Figure Captions List